

pH and Concentration Dependence of Luminescent Characteristics in Glass-Encapsulated Eu-Complex

Eimo Kin, Takeshi Fukuda, Sayaka Kato, Zentaro Honda, and Norihiko Kamata

Graduate School of Science and Engineering, Saitama University,

255 Shimo-Ohkubo, Sakura-ku, Saitama-shi, Saitama 338-8570, Japan

TEL/FAX: +81-48-858-3526

Corresponding author: T. Fukuda e-mail: fukuda@fms.saitama-u.ac.jp

Abstract

In order to improve the stability of red phosphor with efficient and high color-purity characteristics under ultraviolet excitation, we encapsulated Eu(TTA)₃phen by sol-gel derived silica glasses and studied their photoluminescence (PL) characteristics. The dependence of pH values in the starting solution revealed that the process condition should be within the modest region with the optimum pH value around 6 to 7. The PL intensity increased with increasing the concentration of Eu(TTA)₃phen initially, then it showed saturating tendency above 0.6 mol%. An improvement of reliability by the glass encapsulation was exemplified by monitoring the long-term PL intensity under constant UV irradiation. We consider that the glass network carefully prepared by sol-gel process is effective for preventing free oxygen and water from attacking Eu(TTA)₃phen molecule without loss of PL output.

Keyword: sol-gel process, phosphor, Eu-complex, encapsulation, photoluminescence, long-term, stability

1. Introduction

Efficient emissive materials at red, green and blue wavelengths with high reliability have been studied extensively for display and lighting applications up to now. After technological developments of GaN-based light-emitting diodes (LEDs) [1, 2], which cover green, blue and ultraviolet (UV) regions, yellow phosphor excited by the blue LED and red-, green- and blue-phosphors excited by UV-LED became indispensable to assemble white LEDs. As for the latter case for high quality lighting, the improvement of color purity as well as the efficiency and reliability in red phosphors are especially important for practical applications. In comparison with conventional inorganic phosphor materials, light emissive complexes are shown to improve the efficiency due to the increase in the absorption of organic ligands [3]. Among these, the tris(2-thenoyltrifluoroacetato)(1,10-phenanthroline)europium(III) complex [4-8], $\text{Eu}(\text{TTA})_3\text{phen}$ in short, have superior efficiency as well as color purity.

The robustness of organic molecules, however, is lower than that of inorganic materials due to the bond strength of molecules fundamentally, which requires us an urgent way of improving reliability at actual condition. Sol-gel encapsulation [9-12] of organic molecules against ambient oxygen and water by inorganic materials are one of crucial technological issues on an inorganic-organic hybridization [13-16] for improving reliability and widening applications of light emissive materials. Sol-gel process with tetraethoxysilane, $\text{Eu}(\text{TTA})_3\text{phen}$ and polyvinyl butyral has been reported from the viewpoints of ternary optimization and crack reduction [17]. A covalent linking of the Eu-complex to the glass matrix has been accomplished by using 5-(*N,N*-bis-3-(triethoxysilyl)propyl)ureyl-1,10-phenanthroline and diethoxydimethylsilane [18]. Though the dependence of organic ligands and process conditions on the fluorescent spectra and their relative intensities were discussed, little has been known on the absolute value of radiative efficiency and the actual effect of glass encapsulation against an intense UV light irradiation up to now.

In continuation to a successful encapsulation of various ions and polysilanes [19-23], we introduced $\text{Eu}(\text{TTA})_3\text{phen}$ into silica glass by sol-gel process, and investigated the effects of pH values in the starting solution and the concentration on the optical characteristics of the glass-encapsulated $\text{Eu}(\text{TTA})_3\text{phen}$. The internal quantum efficiency was determined as the most direct measure of radiative efficiency, and the improvement of long-term stability was exemplified by monitoring the long-term decrease in photoluminescence (PL) intensity under a constant UV light excitation at 400 nm. Combining superior efficiency and functionality of rare-earth complexes with transparent and protective glass matrix opens a wider field of effective inorganic-organic hybridized materials.

2. Experimental

2.1 Eu-Complex for UV-LED Excitation

We selected $\text{Eu}(\text{TTA})_3\text{phen}$, shown in the insert of Fig. 1, as the efficient red-phosphor with high color purity for the 400 nm excitation. The PL excitation (PLE) spectrum, however, depends on the local configuration of the complex. The original $\text{Eu}(\text{TTA})_3\text{phen}$ powder was dissolved in *N,N*-Dimethylformamide (DMF) with a concentration of 1 mg/ml, and was spin-coated at 1500 rpm for 1 min. Figure 1 shows PL and PLE spectra of the original $\text{Eu}(\text{TTA})_3\text{phen}$ powder and the spin-coated film. The PL spectrum was measured by the excitation at 400 nm, and the PLE spectrum was monitored at 612 nm. Though the original powder showed distinct PLE intensity at 400 nm, the absorption edge of the spin-coated film was shifted to the shorter wavelength side, making it difficult to excite by the same wavelength.

This spectral change was observed also in solutions and was attributed to the difference in molecular conformation of the $\text{Eu}(\text{TTA})_3\text{phen}$. In the original powder, the $\text{Eu}(\text{TTA})_3\text{phen}$ molecule stacks each other within a size of a microcrystalline, forming a stacked molecular conformation. In a spin-coated film, on the other hand, such stacked order or symmetry disappears and $\text{Eu}(\text{TTA})_3\text{phen}$ molecules are randomly oriented with a variety of pores among them. The situation is considered to be similar to a relaxed conformation in a good solvent.

2.2 pH Dependence

In order to observe the pH dependence, we dissolved $\text{Eu}(\text{TTA})_3\text{phen}$ into the mixture of DMF and deionized water so that the concentration of the Eu-complex became 1.0×10^{-7} mol/ml. The volume ratio of DMF:water was 1:1. Then a small amount of nitric acid or ammonia water was added to control the pH value of the solution. Figure 2(a) shows two examples of both PL and PLE spectra of the solution at pH values of 5 and 6. Here wavelengths of excitation in PL and of emission in PLE were 380 nm and 612 nm, respectively. The shift of the absorption edge toward

shorter wavelength side was common to that of a spin-coated film shown in Fig. 1. The PL intensity increased with increasing the pH value from 3 to 6, but it decreased down to one tenth at the pH value of 7. In case the $\text{Eu}(\text{TTA})_3\text{phen}$ concentration was set at 5.0×10^{-7} mol/ml, the shape of the PLE was similar to that at lower concentration as examples shown in Fig. 2(b). The PL intensity, however, reached its maximum value at $\text{pH}=7$, and it decreased down at $\text{pH}=8$ drastically. There existed a distinct concentration dependence.

In order to consider these data, absorption spectra of these solutions for both cases of 1.0×10^{-7} and 5.0×10^{-7} mol/ml were measured at the same time. The absorbance at 330nm wavelength and the normalized PL intensity were plotted as a function of pH values, as shown in Figs. 3(a) and (b), respectively. The absorption was weak at acidic side around $\text{pH}=3$ especially in the thinner solution, corresponding to the weak PL intensity. Both the PL intensity and the absorbance increased with increasing pH value from 5 to 6 in the thinner solution, however, there were no correlation between them above pH value of 7. The absorbance of the thicker solution showed no distinct change at the pH value between 4 and 9 unlike the steep change of the PL intensity peaked at $\text{pH}=7$. The nearly constant absorbance between 4 and 9 was not due to saturation of experimental apparatus. It should be noticed that the decomposition of the ligand takes place at strongly acidic condition rather than that at basic condition. The concentration of $\text{Eu}(\text{TTA})_3\text{phen}$ itself affects the decomposition. It is clear that the absorbed energy above the pH value of 8 was bypassed through non-radiative recombination processes. These results indicate that the optimum pH condition in the starting solution is moderate one as previously reported [18], around the pH values of 6 to 7, depending on the concentration of $\text{Eu}(\text{TTA})_3\text{phen}$.

2.3 Preparation of sol-gel silica glass

The conventional sol-gel method [24, 25] is based on hydrolysis and condensation of organoalkoxides as starting materials with the aid of catalyst, water and alcohol. Since the solution is homogeneous and the condition of such chemical synthesis is mild without the need for high temperature process [26, 27], it provides a versatile way of introducing organic molecules, thus fabricating inorganic-organic hybridized functional materials.

Since many alkyl- or phenyl-silsesquioxane gels derived from alkoxy silane have flexible structures with the low-softening temperature (from tens to 200°C at most), numerous silica- and/or siloxane-based hybrid materials have been investigated in the past few years [14]. Easy casting and patterning of the fabrication process is utilized for industrial coatings on various substrates, exploiting combinations for good adhesion, corrosion protection, transparency, tunable refractive-index, improvement of mechanical properties etc.

Starting solution of tetramethoxysilane (TMOS), ethanol, deionized w

$\text{Eu}(\text{TTA})_3\text{phen}$ at each concentration was collected into a quartz glass cell. PL and PLE spectra were measured at RT by a spectrofluorometer (HORIBA Jovin Yvon, FluoroMax-3), of which excitation source was the combination of a 150W Xenon arc-lamp and a monochromator. The absorbance was also measured at RT by a double-beam UV-Vis spectrophotometer (JASCO, V550). In order to estimate the long-term stability, we recorded the normalized PL intensity as a function of time under UV irradiation by a spectrofluorometer (HORIBA Jovin Yvon, FluoroMax-3). The center wavelength and the optical intensity were 400 nm and 2.33 mW/cm^2 , respectively.

3. Results and Discussion

3.1 Concentration Dependence

The luminous transition of $\text{Eu}(\text{TTA})_3\text{phen}$ originates from ${}^5\text{D}_0 \rightarrow {}^7\text{F}_J$ ($J=1, 2, 3, 4$) in Eu^{3+} [18, 28-29]. All the glass encapsulated $\text{Eu}(\text{TTA})_3\text{phen}$ samples showed a distinct peak of ${}^5\text{D}_0 \rightarrow {}^7\text{F}_2$ transition of 612 nm in the PL spectrum, as shown in Fig. 4, resulting in the high color-purity as a red component. Absorption tails of the PLE spectra were similar to those of the original powder shown by the solid curve in Fig. 1, having a sufficient intensity for the 400nm excitation. Note that this result was due to the stacked conformation of $\text{Eu}(\text{TTA})_3\text{phen}$ by selecting the poor solution of ethanol and water.

Glass-encapsulated samples were packed into standard glass cells, and their PL spectra were measured under the excitation of 400 nm at the fixed incident angle. In order to evaluate the absolute efficiency of PL at the same time, the internal quantum efficiency was measured by a luminance quantum yield measurement system (Systems Engineering Inc., QEMS-2000) with the following scheme: First, a standard diffuser was set at the sample position of an integrating sphere and was irradiated by an LED with the peak wavelength of 400nm. The intensity of the excitation light from an observation window of the integrating sphere was transferred through an optical fiber, fed to a monochromator with a CCD array, and was recorded in a computer. Next,

the glass-encapsulated $\text{Eu}(\text{TTA})_3\text{phen}$ was placed on a glass plate at the sample position, and was irradiated by the same excitation light. The PL of the sample and the residual intensity of the excitation light as a result of sample absorption from the same observation window were fed to and resolved spectroscopically by the same detection system. After fitting each observed spectral curve in the computer, the value of internal quantum efficiency was determined as the photon number ratio of the PL to the absorption in the calibrated integrating sphere system.

Figure 5 shows the concentration dependence of the PL intensity normalized by that of the original $\text{Eu}(\text{TTA})_3\text{phen}$ powder packed in the same cell and the internal quantum efficiency of glass-encapsulated $\text{Eu}(\text{TTA})_3\text{phen}$. The normalized PL intensity increased with increasing concentration up to 0.6 mol%, then tended to saturate. It should be noticed that even the glass-encapsulated sample of 0.6 mol% showed a comparable PL intensity relative to $\text{Eu}(\text{TTA})_3\text{phen}$ powder itself. Values of the internal quantum efficiency were higher than 55 % in the experimental range, as shown in Fig. 5. Thus the concentration dependence of the normalized PL intensity was attributed to the amount of absorption in the standard cell used in the experiment. This result leads us an optimistic forecast on the application of glass-encapsulated $\text{Eu}(\text{TTA})_3\text{phen}$ as a possible inorganic-organic hybridized phosphor materials.

3.2 Stabilization of $\text{Eu}(\text{TTA})_3\text{phen}$ by Sol-Gel Glass

We compared a long-term stability of relevant materials by monitoring the temporal variation of PL intensities under constant UV excitation. The excitation light of 400nm wavelength with the density of 2.33 mW/cm^2 irradiated each sample in various ambient, and the PL intensity at the peak wavelength of 612 nm, normalized by its initial one, was plotted in Fig. 6.

The spin-coated $\text{Eu}(\text{TTA})_3\text{phen}$ film showed no PL degradation in vacuum, however 23 % decrease in air after the UV irradiation of 90 min. The difference is attributed to the decomposition or oxidation of ligand bonding due to oxygen and/or water in air. The glass-encapsulated $\text{Eu}(\text{TTA})_3\text{phen}$, on the other hand, showed no distinct decrease even in air. The superiority of the stability over original $\text{Eu}(\text{TTA})_3\text{phen}$ powder is also clear as shown in Fig. 6.

During sol-gel process, primary particles are formed in the starting solution and then they agglomerate each other to form secondary particles. Many pores in a variety of scales ranging from nm to μm , therefore, might be formed in sol-gel derived glass networks without heat treatment over 800°C . Nevertheless, these results exemplified the effect of encapsulation against free oxygen and water by glass network treated at most 100°C , due to the careful consideration for preventing molecular degradation during sol-gel process.

4. Conclusions

We encapsulated an efficient and high color-purity red phosphor material, $\text{Eu}(\text{TTA})_3\text{phen}$, into sol-gel silica glass, and investigated its optical properties based on PL and PLE spectroscopy and the internal quantum efficiency. A successful encapsulation and stabilization, capable of using excitation light of 400 nm wavelength, was confirmed by controlling process conditions including pH value and $\text{Eu}(\text{TTA})_3\text{phen}$ concentration in the starting solution. The PL intensities of the glass-encapsulated $\text{Eu}(\text{TTA})_3\text{phen}$ showed a superior long-term stability against UV light excitation without lowering the absolute value of light output. The method opens a field of effective inorganic-organic hybridized materials, combining superior functionality of organic molecules with transparent and protective nature of glass matrix.

Acknowledgements

The authors would like to thank Dr. K. Okaniwa (Hitachi Chemical Co. Ltd.) for providing $\text{Eu}(\text{TTA})_3\text{phen}$ powders.

References

1. Nakamura S, Senoh M, Iwasa N (1995) *Jpn J Appl Phys* 34:1332
2. Nakamura S (1998) *Science* 281:956
3. Reisfeld R. (1984) *J Electrochem Soc* 131:1360
4. Matthews LR, Knobbe ET (1993) *Chem Mater* 5:1697
5. Li H, Inoue S, Machida K, Adachi G (1999) *Chem Mater* 11:3171
6. Ling Q, Yang M, Wu Z et al (2001) *Polymer* 42:4605

7. Fang J, Ma D (2003) *Appl Phys Lett* 83:4041
8. Vaganova E, Reisfeld R, Yitzchaik S (2003) *Opt Mater* 24:69
9. Ellerby LM, Nishida CR, Nishida F et al (1992) *Science* 255:1113
10. Klein LC (1993) *Annu Rev Mater Sci* 23:437
11. Wang Y, Caruso F (2005) *Chem Mater* 17:953
12. Aslam M, Fu L, Li S (2005) *J Colloid Interface Sc* 290:444
13. Sanchez C, Ribot F (1994) *New J Chem* 18:1007
14. Livage J (1999) *Bull Mater Sci* 22:201
15. Gupta R, Chaudhury NK (2007) *Biosens Bioelectron* 22:2387
16. Li F, Li J, Zhang SS (2008) *Talanta* 74:1247
17. Fu L, Zhang H, Wang S et al (1999) *J Sol-Gel Sci Technol* 15:49
18. Binnemans K, Lenaerts P, Driesen K et al (2004) *J Chem.* 14:191
19. West R (1986) *J Organomet Chem* 300:327
20. Kamata N, Satoh C, Tosaka K, Yamada K. (2001) *J Non-Cryst Solids* 595:293
21. Satoh H, Kamata N, Kanezaki K et al (2001) *Springer Proc in Physics* 87:1669
22. Kamata N, Ishii R, Tonsyo S et al (2002) *Appl Phys Lett* 81:4350
23. Kamata N, Terunuma D, Ishii R et al (2003) *J Organomet Chem* 685:235
24. Stręk W, Sokolniciki J, Legendzieicz J et al (1999) *Opt Mater* 13:41
25. Pawlik EM, Stręk W, Deren PJ et al (1999) *Spectrochim Acta A* 55:369
26. Liu DM, Troczynski T, Tseng WJ (2001) *Biomaterials* 22:1721
27. Gill I, Ballesteros A (2000) *Trends in Biotechnology* 18:282
28. Eilers H, Tissue BM (1996) *Chem Phys Lett* 251:74
29. Pereira P, Caiut J, Ribeiro S et al (2007) *J Lumin* 126:378

Figure captions

Fig. 1. PL and PLE spectra of original $\text{Eu}(\text{TTA})_3\text{phen}$ powder (solid curve) and spin-coated $\text{Eu}(\text{TTA})_3\text{phen}$ film (dashed curve). Monitored wavelength of the PLE and excitation wavelength of the PL were 612 and 400 nm, respectively. The molecular structure of $\text{Eu}(\text{TTA})_3\text{phen}$ is shown in the insertion.

Fig. 2 Dependence of the pH value on PL and PLE spectra in the DMF and H_2O (1:1) solution of $\text{Eu}(\text{TTA})_3\text{phen}$ at (a) 1.0×10^{-7} mol/ml and (b) 5.0×10^{-7} mol/ml.

Fig. 3 (a) The absorbance at 330nm and (b) the normalized PL intensity in the DMF and H_2O (1:1) solution of $\text{Eu}(\text{TTA})_3\text{phen}$ as a function of the pH value.

Fig. 4 PL and PLE spectra of the glass-encapsulated $\text{Eu}(\text{TTA})_3\text{phen}$ with its concentration as a parameter.

Fig. 5 The normalized PL intensity (solid curve) and the internal quantum efficiency (dashed curve) of glass-encapsulated $\text{Eu}(\text{TTA})_3\text{phen}$ as a function of its concentration.

Fig. 6 The temporal variation of the normalized PL intensity under 400 nm excitation. The excitation density was 2.33 mW/cm^2 .

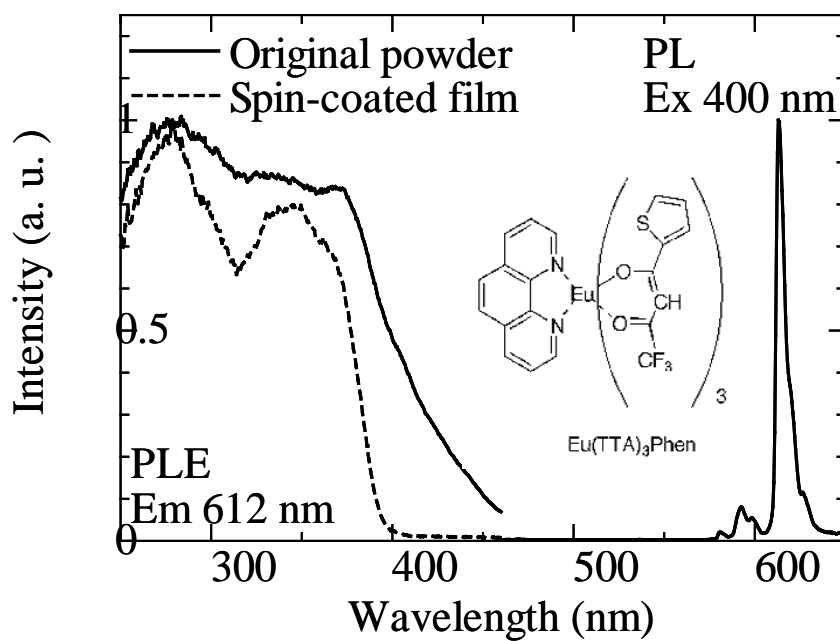


Fig. 1. PL and PLE spectra of original $\text{Eu}(\text{TTA})_3\text{phen}$ powder (solid curve) and spin-coated $\text{Eu}(\text{TTA})_3\text{phen}$ film (dashed curve). Monitored wavelength of the PLE and excitation wavelength of the PL were 612 and 400 nm, respectively. The molecular structure of $\text{Eu}(\text{TTA})_3\text{phen}$ is shown in the insertion.

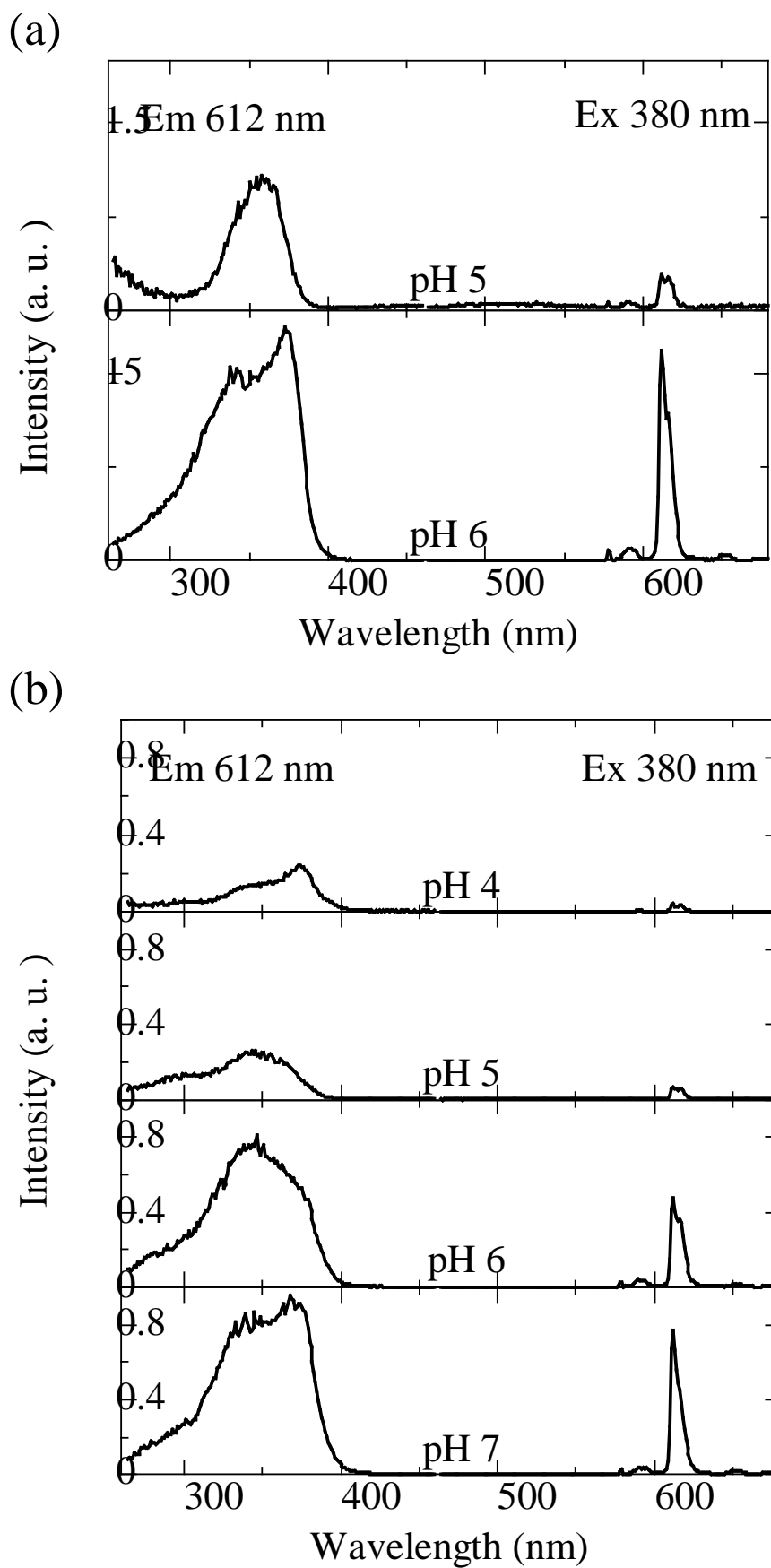


Fig. 2 Dependence of the pH value on PL and PLE spectra in the DMF and H₂O (1:1) solution of Eu(TTA)₃phen at (a) 1.0×10^{-7} mol/ml and (b) 5.0×10^{-7} mol/ml.

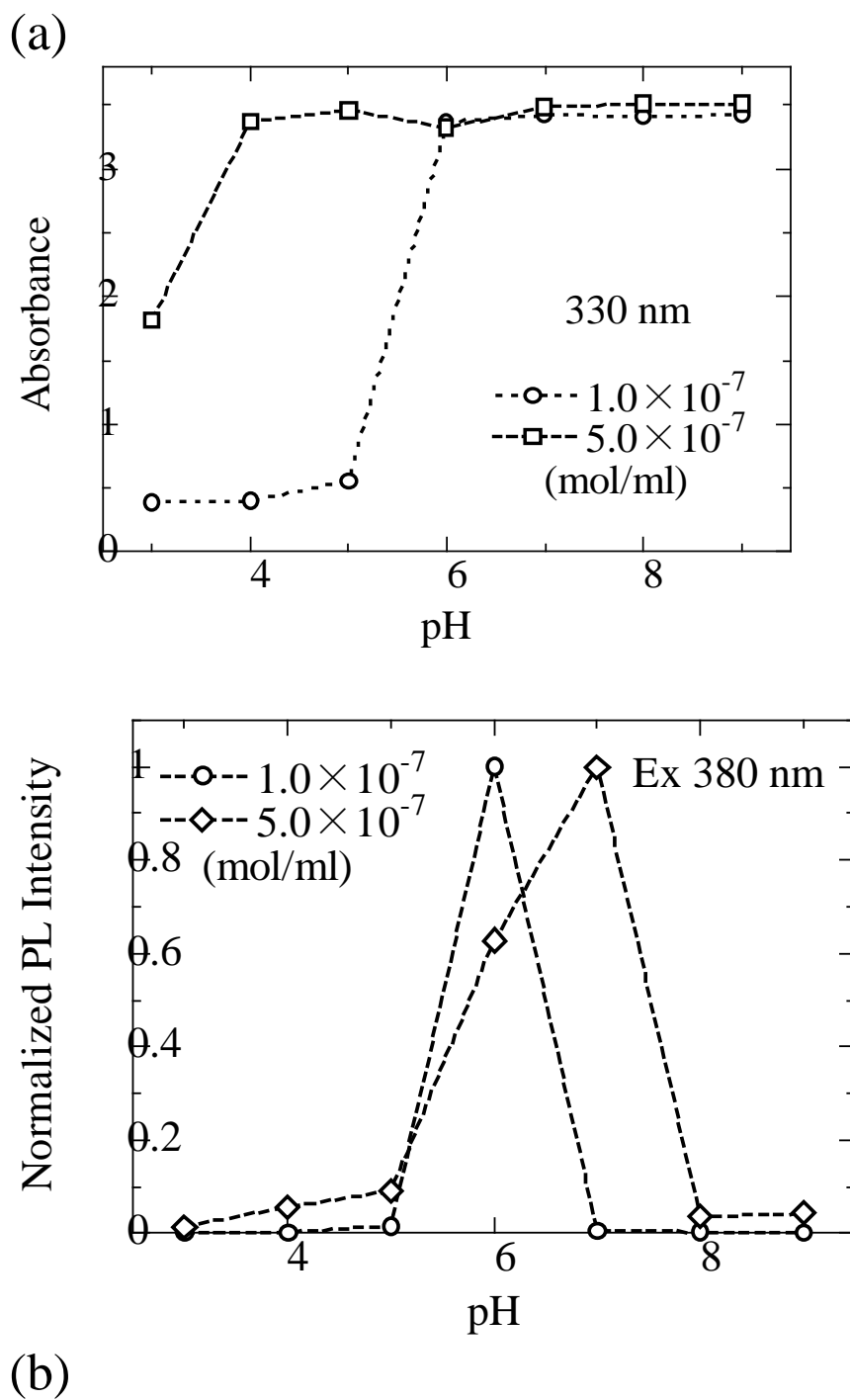


Fig. 3 (a) The absorbance at 330nm and (b) the normalized PL intensity in the DMF and H₂O (1:1) solution of Eu(TTA)₃phen as a function of the pH value.

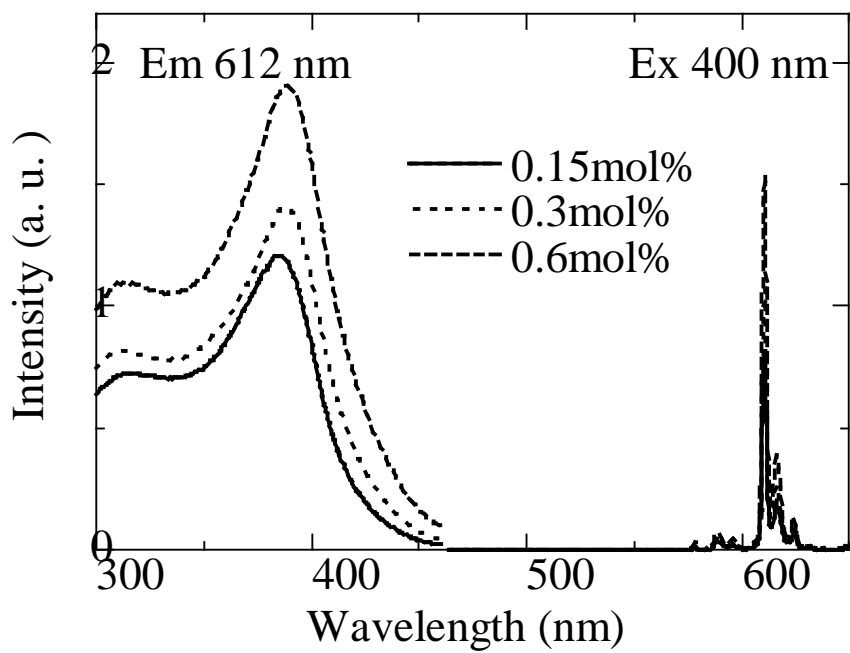


Fig. 4 PL and PLE spectra of the glass-encapsulated Eu(TTA)₃phen with its concentration as a parameter.

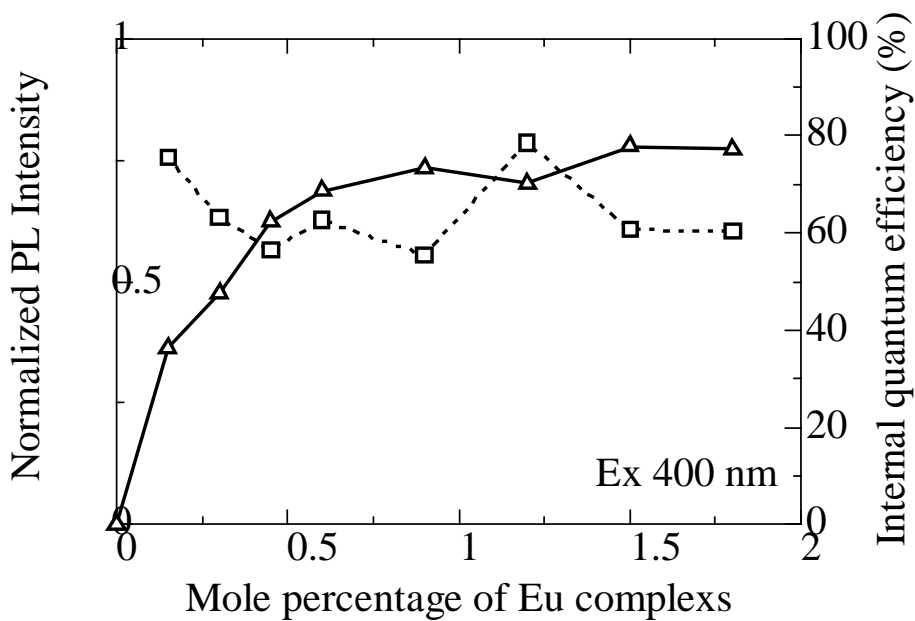


Fig. 5 The normalized PL intensity (solid curve) and the internal quantum efficiency (dashed curve) of glass-encapsulated Eu(TTA)₃phen as a function of its concentration.

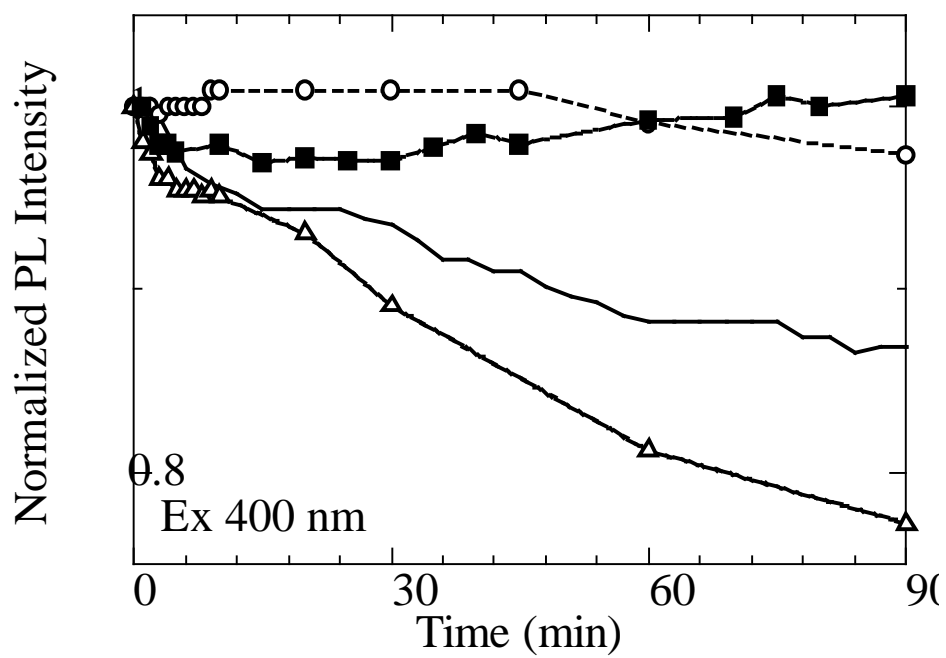


Fig. 6 The temporal variation of normalized PL intensity under 400 nm excitation. The excitation density was 2.33 mW/cm^2 .

■ glass encapsulated sample in air △ spin-coated film in air
 — original powder in air ○ spin-coated film in vacuum